Talanta 99 (2012) 369–374

Contents lists available at SciVerse ScienceDirect

Talanta

journal homepage: www.elsevier.com/locate/talanta

Analysis of rare earth elements in seawater by inductively coupled plasma mass spectrometry after pre-concentration using TSK^{TM}-HD-MW-CNTs (highly dispersive multi-walled carbon nanotubes)

Juhye Cho [a], Kwang-wha Chung [a,*], Man Sik Choi [a,b,**], Hae-jin Kim [a,c]

[a] Graduate School of Analytical Science and Technology, Chungnam National University, Daejeon 305-764, Republic of Korea
[b] Department of Ocean Environmental Sciences, Chungnam National University, Daejeon 305-764, Republic of Korea
[c] Division of Nano-material Science, Korea Basic Science Institute, Daejeon 305-333, Republic of Korea

ARTICLE INFO

Article history:
Received 22 March 2012
Received in revised form
29 May 2012
Accepted 30 May 2012
Available online 7 June 2012

Keywords:
Rare earth elements
Seawater
Multi-walled carbon nanotube
ICP/MS
Pre-concentration

ABSTRACT

This study aimed to identify easy-to-use multi-walled carbon nanotubes (MW-CNTs) having a high capacity to adsorb metals and thereby expand the usability of these materials as a solid-phase adsorbent for the analysis of trace metals in seawater. High-dispersion-type MW-CNTs had the highest metal binding capacity (70.8 ± 5.1 mg/g for La) after a strong acid oxidation procedure, possibly because the high dispersibility resulted in a more complete reaction than with highly crystalline types. Because the high-dispersion-type MW-CNTs leaked from a conventional column, they were attached to polymer beads (TSK^{TM}) (pore diameter about 20 μm). Flow rate, pH, and volume of the seawater sample, as well as eluent type and volume, were optimized to obtain 0.01–0.16 pg/mL detection limits for rare earth elements (REEs). In addition, normalized patterns for samples collected from the East Sea showed characteristic features of REEs in seawater, i.e., a negative Ce anomaly, low atomic number REE (LREE) depletion, and high atomic number REE (HREE) enrichment.

1. Introduction

Y and lanthanides, which are called "rare earth elements (REEs)", behave similarly in an aqueous environment because of their similar atomic properties such as ionic size and charge. With the exception of Ce and Eu, REEs have a trivalent oxidation state in seawater but have different particle reactivities and complexing abilities depending on their atomic number [1–3]. This results in the depletion of low atomic number REEs (LREEs) and enrichment in high atomic number REEs (HREEs) in seawater compared to continental rocks [1–3]. Ce and Eu have soluble divalent and insoluble tetravalent oxidation states. The fractionation of LREEs, mid-atomic number REEs (MREEs), and HREEs, and the anomaly with Ce and Eu, enables them to be used as tracers for ocean circulation [1–3] and the origin of terrestrial materials [4], as a probe for investigating the scavenging process of particles [1], and as a proxy for the redox state in ancient oceans [6]. Although REEs are useful tracers for chemical processes in the marine environment and several precise and reliable analytical techniques have been developed [3–5,8–11], the development of more easy and rapid analytical method with high throughput and simple procedure is essential because of their low concentrations in seawater (sub-nanomolar to picomolar levels).

Inductively coupled plasma mass spectrometry (ICP-MS) is commonly used to quantify REEs [2–6] because of its multi-element detection over a wide concentration range with low detection limits, e.g., picomolar. Although REEs in seawater have sub-nanomolar to picomolar concentrations [7,8], pre-concentration and chemical separation of REEs is essential because of the high dissolved salt contents in seawater and for the acquisition of consistent data. Liquid–liquid extraction [9,10], co-precipitation [14], and solid-phase extraction (SPE) [6,11,12] have been used for pre-concentration of ultra-trace REEs and matrix separation in seawater. SPE using column chromatography has several advantages such as high throughput, automation, small sample and reagent quantities, simple procedure, low analyte levels in the blank, and low quantities of wastes.

Recently, carbon nanotubes have been evaluated as sorbents for trace metals, organic pollutants, and biomolecules [13–15]. Multi-walled carbon nanotubes (MW-CNTs), which have large surface area, high mechanical strength, and chemical stability, have been widely used as a solid sorbent for the analysis of Pb, Au, Rh, Mn, Fe, Cu, and REE in samples such as mineral water, serum, synthetic seawater, garlic, and rocks [13,16]. However, van der

* Corresponding author.
** Corresponding author at: Graduate School of Analytical Science and Technology, Chungnam National University, Daejeon 305-764, Republic of Korea.
E-mail addresses: kwchung@cnu.ac.kr (K.-w. Chung), mschoi@cnu.ac.kr (M.S. Choi).

0039-9140/$ - see front matter © 2012 Elsevier B.V. All rights reserved.
http://dx.doi.org/10.1016/j.talanta.2012.05.066

Waals attractions frequently cause CNTs to aggregate into bundles [17], which hinders their usefulness as sorbents in SPE applications. To overcome the aggregation problem and improve dispersibility, oxidation of CNTs by various concentrated acids [17–22], organic peroxide [23], and ozone [24] has been applied. In addition, oxidation enhances the capacity of CNTs to adsorb metals in solution, which is a critical factor for sorbents of metals because higher capacity permits a higher pre-concentration factor in the analysis of trace metals in seawater.

This study aimed to identify CNTs having a higher capacity for metal adsorption. Various types of CNTs were evaluated: highly dispersible, highly crystalline, oxidized, and non-oxidized. We present the analytical merits of REEs in seawater for CNTs having the highest capacity.

2. Materials and methods

2.1. CNTs

Two types of CNTs were purchased from Hanwha Nanotech (Inchon, Korea): CM95 and CM250, which are highly crystalline (HC) and highly dispersive (HD) MW-CNTs, respectively [25,26]. The HC-MW-CNTs are short and entangled, while the HD-MW-CNTs are long, aligned bundles. The absorbance of supernatants after centrifugation was used as the metric for dispersibility; HC types decreased to 40.7%, while HD types remained at 93.4% [25,26].

The CNTs were oxidized using the procedure of Datsyuk et al. (2008). CNTs (5 g) were washed sequentially with acetone and aqueous sodium hydroxide (100 mL for HC type and 150 mL for HD type), and purified water (18.2 MΩ). These pre-treated CNTs were refluxed at 160 °C for 60 min with concentrated HNO_3 and H_2SO_4 (1:3) and then rinsed with purified water until neutral pH. The capacities of the pre-treated non-oxidized and oxidized HD-MW-CNTs and HC-MW-CNTs were measured after oven-drying at 100 °C.

Scanning electron microscopy (SEM, S-4800, Hitachi High-Technologies Co., Tokyo, Japan) and surface area analyzer (ASAP 2020, Micromeritics, Georgia, USA) were used to study the surface morphology, surface area, pore volume, and diameter.

The capacity of each CNT type for the adsorption of La was determined batch-wise. About 30 mg of CNTs were added to 50 mL of a 50 μg/mL La standard solution (ANAPURE, Daejeon, Korea) adjusted to pH 4 using 20% ammonium acetate buffer. The mixed solution was shaken for 2 h and then filtered under vacuum through a 0.45-μm membrane filter. La attached to CNTs was eluted using 10 mL of 2 M HNO_3 solution to check for mass balance. The filtered solution was acidified to pH 1.5 using concentrated HNO_3, and the La content was measured by inductively coupled plasma atomic emission spectrometry (ICP-AES; Perkin Elmer Inc., Optima 4300DV, California, USA).

2.2. Preparation of resin and column

CNTs were usually packed into micro-columns with glass wool at the ends [16,25] and containing polyethylene frits having a nominal pore size of 10–30 μm [26]. Although the column could be used in the usual way with HC-MW-CNTs, HD-MW-CNTs leaked from the column even at low pressure because of their high degree of dispersion. Although a small-pore-size filter (e.g., 0.45-μm filter paper [27]) could be used instead of a column to prevent the leakage of CNTs, in practice it was difficult to filter volumes of seawater larger than 100 mL with a 27-mm-diameter membrane filter.

The attachment of CNTs to large beads (e.g., silica [28]) is another option. Because silica beads can give higher levels of metal in the blank, we chose a vinyl polymer gel, TSK™ (TOYOPEARL HW75F, SUPELCO). This material has been widely used as a support for 8-hydroxyquinoline [29]. CNTs (0.8 g) and TSK™ (5 g) were immersed in about 40 mL of purified water, and the solution was shaken for 24 h. After centrifugation, the supernatant was discarded. Purified water (40 mL) was added to the centrifuge vial; the sample was then shaken and centrifuged to remove unattached CNTs. This step was repeated until the supernatant was almost clear. The quantity of CNTs attached to the TSK™ was determined by gravimetric analysis after oven-drying the TSK™-attached CNTs. However, it was difficult to obtain reliable data because the small CNT bundles could not be separated. Thus, the quantity of CNTs attached to TSK™ was estimated by measuring the adsorption capacity of TSK™, CNTs, and CNTs attached to TSK™ (TSK™-HD-MW-CNT).

TSK™-HD-MW-CNT resin (1.5 mL) was packed into a polypropylene column (8 mm diameter, 5 cm long) having 20-μm polyethylene frits as supports at both ends. Ten columns were run simultaneously using a 12-channel peristaltic pump capable of controlling the water flow rate at 0.1 mL/min.

2.3. Optimization of REE analysis in seawater

The separation of the matrix and the appropriate adsorption/elution of REE are the most important procedures for obtaining reliable REE data in seawater. The optimized conditions for sample pH, sample flow rate, sample volume, and eluent volume and type were determined. To identify the best sample pH for providing maximum REE recovery and the separation of major cations (Na^+, Ca^{2+}, Mg^{2+}), 10 ng/mL standard solutions containing mixed REEs, transition-metal cations, and major cations were prepared from stock solutions (SPEX Certi Prep Co.) and pH was adjusted from 1.6 to 9.5 with appropriate buffer solutions, i.e., phosphoric acid–potassium phosphate, acetic acid–ammonium acetate, ammonium acetate, and ammonia–ammonium acetate. The flow rate was 2 mL/min, and the eluent was 2 M HNO_3 solution. Eluent types (0.1, 0.5, 1, and 2 M HNO_3 or HCl) and volume (1, 2, 3, and 4 mL of 2 M HNO_3) were also evaluated for recovery at a sample pH of 4. The sample flow rate (2, 3, and 5 mL/min) and volume (50, 100, 300, and 400 mL) were tested at a sample pH of 4 and flow rate of 2 mL/min for 2 M HNO_3 eluent.

For the analysis of REEs in seawater, the procedure was as follows: 100 mL of filtered seawater was adjusted to pH 4 with 20% acetic acid–ammonium acetate buffer and passed through the TSK™-HD-MW-CNT column at a flow rate of 2 mL/min using the peristaltic pump. Residual salts in the column were subsequently washed out with 10 mL of purified water. Metals adsorbed onto the resin were eluted using 3 mL of 2 M HNO_3. After mixing of the eluted sample with an internal standard solution having 5 ng/mL of In and Tl (SPEX Certi Prep Co.), the REEs, In, and Tl isotopes were measured using ICP/MS (Thermo Elemental Ltd., X7, Manchester, UK) at the Korean Basic Science Institute (KBSI). Signal drift and suppression by the matrix solution was corrected using the ^{105}In and ^{205}Tl intensities.

The performance of the analytical method for REEs in seawater was evaluated through the estimation of the detection limit, recovery, and precision. The detection limit was determined using seven laboratory procedural blanks each comprising 10 mL of acidified deionized water. Recovery was measured for metal-free seawater samples (seawater after the removal of transition metals and REEs) spiked with REEs in the range of 0.1–200 pg/mL. Precision estimates were established for five replicate measurements of purified seawater spiked with REEs (5 pg/mL). In addition, REEs in actual seawater samples were analyzed and compared to data obtained by another pre-concentration method, i.e., using NOBIAS chelate-PA1 [30].

2.4. Samples

Metal-free seawater was prepared by passing surface seawater collected from the East Sea through a Chelex-100 (Bio-Rad) column having a dimension of 20 cm (length) × 5 cm (diameter). For the analysis of REEs, seawater was collected using a Niskin-type water sampler adapted to sample at seven water depths (50, 100, 200, 400, 600, 800, and 1000 m) at a station (water depth 2200 m) during the 2010 Dokdo oceanographic expedition of the Korean Ocean Research and Development Institute (KORDI). Bulk seawater samples were acidified by concentrated HNO_3 and stored until analysis.

3. Results and discussion

3.1. Characterization of HD-MW-CNTs

Surface properties, including the external shape by SEM imaging, specific surface area by the BET (Brunauer, Emmett and Teller) method (S_{BET}), external surface area (S_{ext}), total pore volume (V_{tot}), micro-pore volume (V_{mic}), and average pore diameter (D_{avg}), were investigated for oxidized/non-oxidized HC-MW-CNT (CM-95) and HD-MW-CNT (CM-250). The results are summarized in Table 1. The adsorption capacities for La of these four types of nanotubes are also listed in Table 1.

Table 1
Surface properties and La adsorption capacity of non-oxidized and oxidized HC-MW-CNTs and HD-MW-CNTs.

	Samples	S_{BET} (m^2/g)	S_{ext} (m^2/g)	V_{tot} (cm^3/g)	V_{mic} (cm^3/g)	D_{avg} (nm)	Capacity (mg/g)
Non-oxidized	HCMWCNT	221	200	1.33	0.019	24.1	3.8 ± 1.0[a]
	HDMWCNT	205	199	1.13	0.013	21.9	5.3 ± 1.2[a]
Oxidized	HCMWCNT	220	199	1.27	0.016	23.1	21.5 ± 4.0[a]
	HDMWCNT	194	175	0.7	0.01	14.4	70.8 ± 5.1[a]

S_{BET}: BET specific surface area, S_{ext}: External surface area, V_{tot}: Total pore volume, V_{mic}: Micropore volume, D_{avg}: Average pore diameter.

[a] Triplicates.

At 100,000 magnification (SEM), the HD-MW-CNTs (about 100–200 nm in length) were longer and straighter than HC-MW-CNTs in the non-oxidized forms (Fig. 1). Oxidized HC-MW-CNTs were shorter than the non-oxidized forms, but oxidation did not change the shape of the HD-MW-CNTs. Because HC-MW-CNTs have a winding shape while HD-MW-CNTs are straight, defects generated during the oxidation process using strong acids might make the HC-MW-CNTs more susceptible to breakage than the HD-MW-CNTs [26]. The specific surface area (S_{BET}) for the four types of nanotubes ranged from 193.6 to 220.9 m^2/g and was slightly higher for oxidized and highly dispersed nanotubes than the non-oxidized and highly crystalline nanotubes. Other properties, such as S_{ext}, V_{tot}, V_{mic}, and D_{avg}, did not show significant differences between the nanotube types.

The adsorption capacities for La of the non-oxidized HC-MW-CNTs and HD-MW-CNTs were 3.8 ± 1.0 mg/g and 5.3 ± 1.2 mg/g, respectively, while those of the oxidized nanotubes were 21.5 ± 4.0 mg/g and 70.0 ± 5.1 mg/g, respectively, which was about an order of magnitude higher than that reported in a previous study [10]. Although the adsorption capacities of the various non-oxidized nanotubes did not differ significantly, the oxidation process greatly increased the adsorption capacity of both types of nanotubes. Oxidation increased the adsorption capacity of the HC-MW-CNTs by about six-fold and of the HD-MW-CNTs by about thirteen-fold. Because the oxidation process did not significantly change the physical properties, the production of binding sites or functional ligands did not seem to be related to the change in physical properties such as increased specific surface area. Furthermore, because the HC-MW-CNTs were shorter than the HD-MW-CNTs due to breakage of the

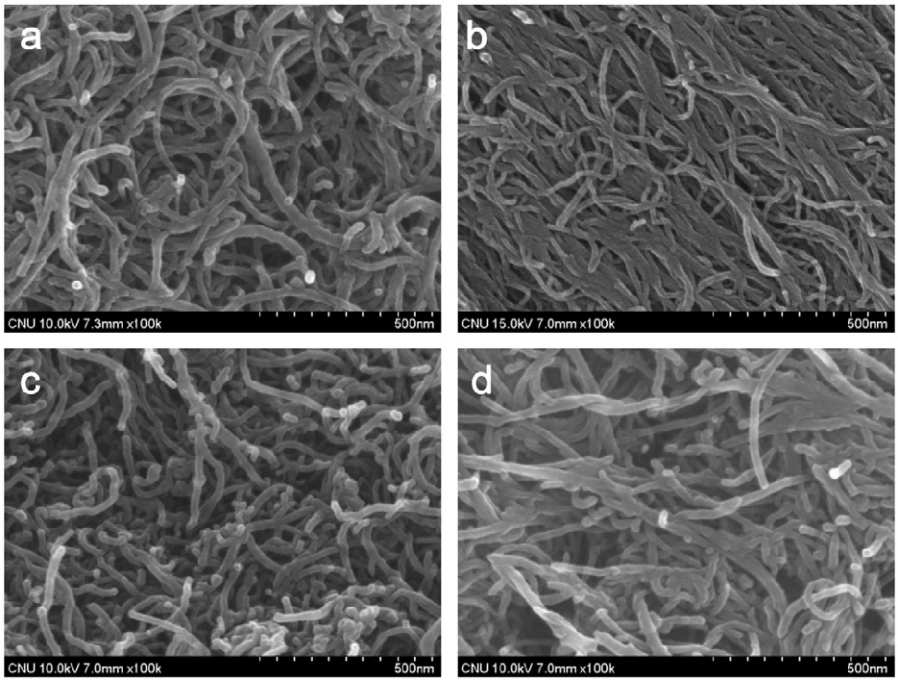

Fig. 1. SEM images for HC-MW-CNTs and HD-MW-CNTs. (a) Non-oxidized HC-MW-CNTs, (b) non-oxidized HD-MW-CNTs, (c) oxidized HC-MW-CNTs, and (d) oxidized HD-MW-CNTs.

winding-shaped CNTs during the oxidation process, the size of the nanotubes did not seem to account for the increased adsorption capacity. Thus, the dramatic increase in the adsorption capacity of oxidized HD-MW-CNTs compared to HC-MW-CNTs is attributed to the enhanced dispersion of the non-oxidized nanotubes. That is, the highly dispersive nanotubes might have reacted more efficiently with the strong acid than the highly crystalline nanotubes.

The quantity of nanotubes in the TSK^{TM}-HD-MW-CNT was estimated using the adsorption capacities for La of TSK^{TM}, HD-MW-CNTs, and TSK-HD-MW-CNT. The percentage of nanotubes in TSK-HD-MW-CNT was 3.65 wt%; thus, the amount of nanotubes was about 30 mg when the 1.5-mL TSK-HD-MW-CNT column was used.

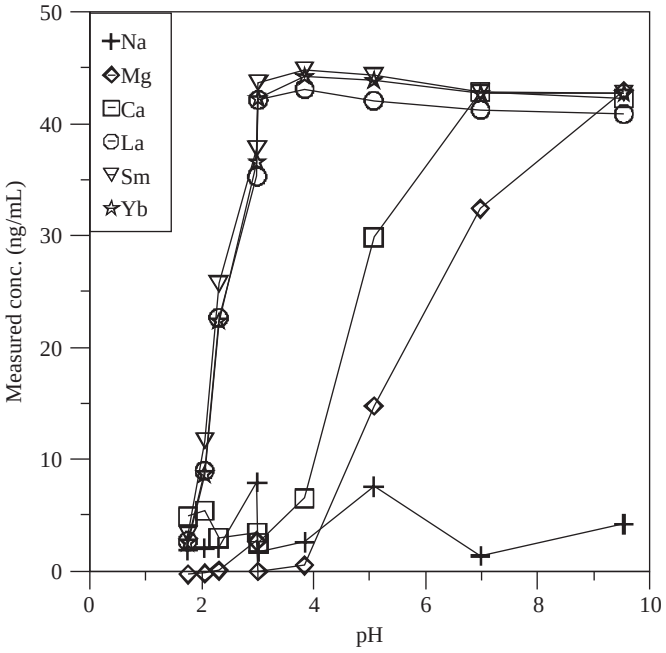

Fig. 2. Breakthrough graphs of matrix cations (Na^+, Mg^{2+}, Ca^{2+}) and REEs (La, Sm, Yb) relative to sample pH.

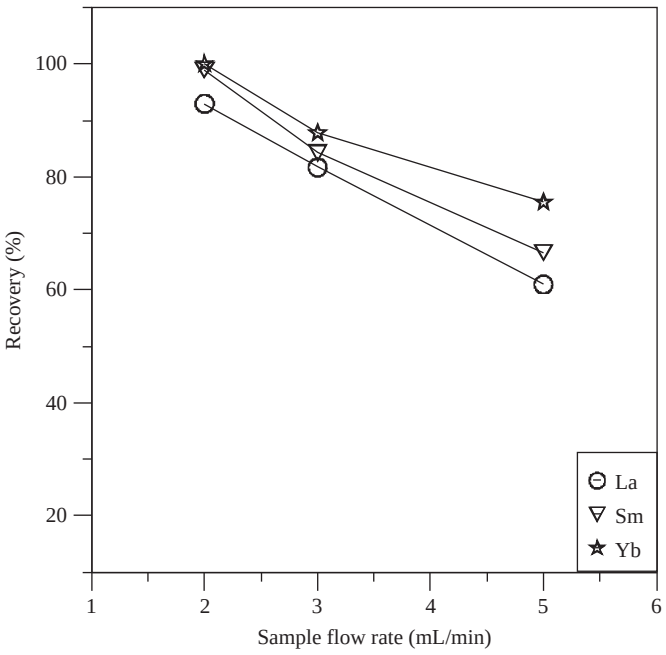

Fig. 3. Recovery percentages of La, Sm, and Yb.

3.2. Optimization of REE analysis in seawater

The eluted concentrations of La, Sm, and Yb as well as those of the matrix cations (Na^+, Ca^{2+}, Mg^{2+}) are presented as a function of sample pH in Fig. 2. Below pH 2, recoveries of all the metals were less than 20%. Increasing the sample pH from 2 to 3 greatly improved the recoveries of La, Sm, and Yb. REEs had maximum recoveries at a sample pH between 3 and 5 and slightly lower recoveries above pH 5. Ca and Mg recoveries increased rapidly from pH 4 to pH 7 or 9, but Na recovery did not show any trend; all had recoveries of less than 20%. Based on metals and matrix cations recoveries, we chose to optimize REE adsorption and separation of the matrix metals at pH 4 and a sample flow rate

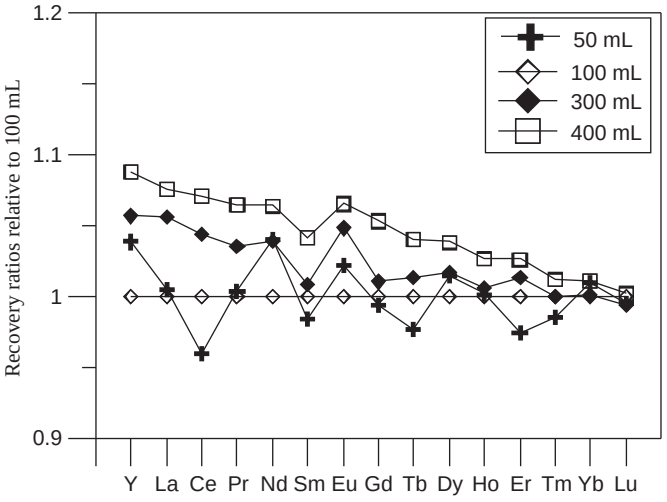

Fig. 4. Recovery ratios of REEs relative to 100 mL seawater sample.

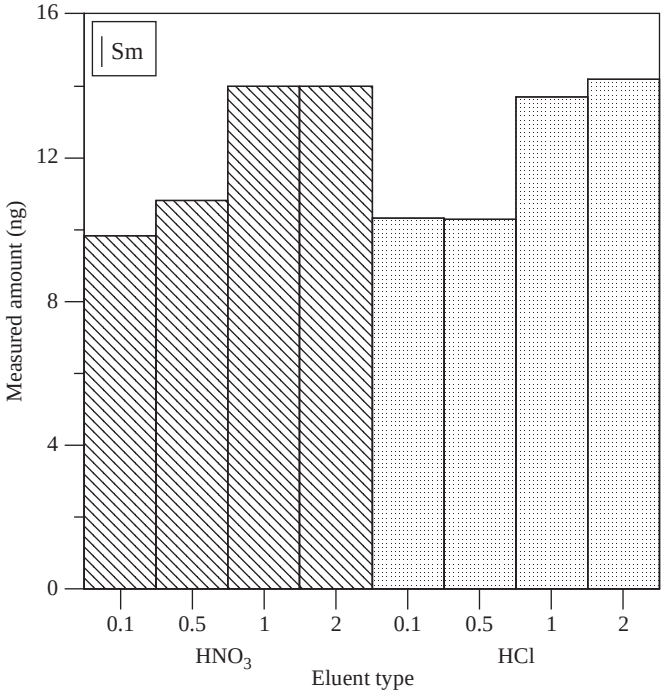

Fig. 5. Recovered concentrations depending on eluent type (HCl and HNO_3) and acid concentration (01, 0.5, 1, and 2 M).

of 2 mL/min; the recoveries of REEs decreased at higher flow rates (Fig. 3).

The dependence of REE recoveries on the volume of seawater used to separate matrix cations was evaluated using 50, 100, 300, and 400 mL of metal-free seawater spiked (0.1 ng/mL) with REEs (Fig. 4). The recoveries of REEs are presented relative to those for 100 mL volumes. Although the recoveries of REEs relative to the spiked quantities ranged from 87% to 108% (not drawn), they decreased gradually from La to Lu with increasing atomic mass. Furthermore, using higher seawater volumes increased the recoveries of La and Sm by as much as 8% (La) and 4% (Sm) for 400 mL samples, while those of Yb were within 1% of each other at all sample volumes. Although the reason why the recovery percentages of La and Sm increased with higher seawater volume was not exactly identified, signal enhancement during ICP-MS measurement might be a plausible explanation due to high matrix cations contents with higher seawater volume.

The acid concentration and type and volume of eluent were determined based on the recoveries for REEs, as presented for Sm (Fig. 5). The maximum recoveries were obtained using 2 M HCl and 2 M HNO_3; 3 mL of 2 M HNO_3 eluted more than 98% of the metals.

Table 2
Limit of detection estimated using procedure blanks.

Elements	Mean[a] (pg/ml)	Std. dev. (pg/ml)	LOD (pg/ml)
Y	3.01	0.42	0.038
La	4.6	1.48	0.135
Ce	5.3	1.75	0.159
Pr	6.1	0.37	0.034
Nd	13.6	1.04	0.095
Sm	2.35	0.31	0.028
Eu	2.11	0.28	0.026
Tb	2.10	0.31	0.028
Gd	1.69	0.20	0.018
Dy	2.49	0.36	0.032
Ho	1.56	0.20	0.018
Er	1.51	0.29	0.027
Tm	1.50	0.24	0.021
Yb	1.70	0.27	0.024
Lu	1.56	0.17	0.016

[a] $n=7$.

3.3. Figure of merits

The concentration limit of detection was calculated as three times the standard deviation for seven laboratory procedural blank solutions divided by the average concentration factor of 33.3, as summarized in Table 2. It ranged from 0.016 (Lu) to 0.159 pg/mL (Ce), which is about 2–10% of the concentration of REEs in real seawater. A higher concentration of Nd relative to the other REEs in the blank solutions was frequently observed, which might be related to intrinsic properties of the CNTs. However, these high Nd levels in the blank solutions did not affect the analytical quality of the REE data in seawater because of the relatively higher natural abundance of Nd.

Five replicate analyses of REEs in 5 pg/mL-spiked seawater had a relative variability of about 2–5%. The measured concentrations were compared with the spiked concentrations using standard addition of REEs from 0.1 to 200 pg/mL in metal-free seawater (Fig. 6). The linear regression equations and coefficients of variance are listed in Table 3. All REE samples showed good agreement between the measured and spiked concentrations, and their mean recoveries were in the range of $93 \pm 2\%$ (La) to $102 \pm 1\%$ (Tm). However, although the high correlation coefficients and small errors of the slope for the regression equations resulted from the samples with much higher concentrations of REEs relative to real seawater, and reproducibility of recoveries might be overestimated, it might be suggested that this method be applicable to samples with a wide range of REE concentrations. When the concentration range of 1–10 pg/ml in LREE and 0.1–1 pg/ml in HREE like in real seawater were considered, about 10% coefficient of variability for mean recoveries could be obtained. Although nearly all the REEs in the metal-free seawater were removed during the Chelex-100 purification step, small amounts of LREE (La to Nd) remained and were then corrected for in the calculation of mean recoveries.

3.4. Seawater collected from the East Sea

Depth profiles of REE concentrations in the East Sea were obtained using HD-MW-CNT pre-concentration and ICP-MS measurements. Seawater samples were collected in August 2007 at 10 water depths from 20 m to 1000 m using a Niskin-type water sampler. The same seawater samples were also analyzed for REEs by NOBIAS chelate-PA1 pre-concentration and ICP-MS measurements [30]. The two data sets were compared through their

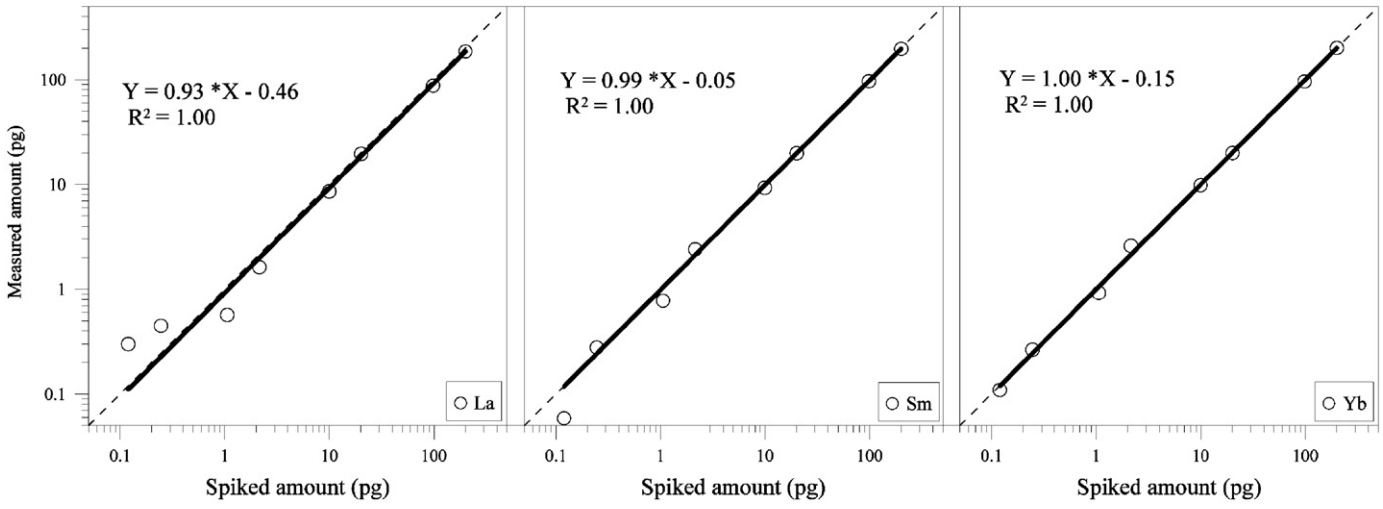

Fig. 6. Measured amounts relative to spiked amounts (0.1–200 pg) for La, Sm, and Yb. The regression lines were drawn according to the equations in Table 3.

Table 3
Regression equations for measured amounts relative to spiked amounts.

Elements	Regression equation	R^2
Y	$Y=0.98(\pm0.01)X+0.30(\pm0.37)$	1.00
La	$Y=0.93(\pm0.02)X-0.22(\pm1.52)$	1.00
Ce	$Y=0.95(\pm0.01)X-0.18(\pm0.40)$	1.00
Pr	$Y=0.96(\pm0.02)X-0.41(\pm1.20)$	1.00
Nd	$Y=0.93(\pm0.05)X-1.99(\pm4.20)$	0.99
Sm	$Y=0.99(\pm0.00)X-0.00(\pm0.30)$	1.00
Eu	$Y=0.99(\pm0.01)X+0.00(\pm0.68)$	1.00
Gd	$Y=0.99(\pm0.02)X-0.05(\pm1.30)$	1.00
Tb	$Y=1.00(\pm0.01)X+0.07(\pm0.40)$	1.00
Dy	$Y=0.99(\pm0.02)X-0.57(\pm1.56)$	1.00
Ho	$Y=1.00(\pm0.01)X+0.28(\pm0.50)$	1.00
Er	$Y=1.00(\pm0.02)X-0.15(\pm1.26)$	1.00
Tm	$Y=1.02(\pm0.01)X-0.05(\pm0.98)$	1.00
Yb	$Y=1.00(\pm0.01)X-0.15(\pm1.07)$	1.00
Lu	$Y=1.01(\pm0.02)X-0.11(\pm1.40)$	1.00

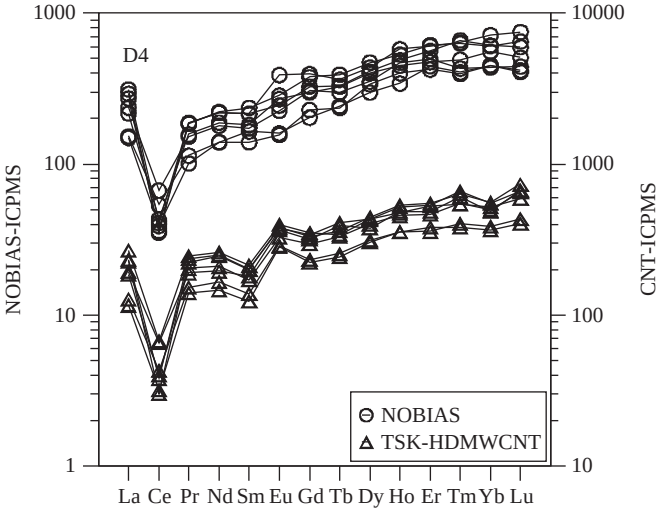

Fig. 7. UCC-normalized REE patterns for seawater collected from the East Sea. Data from TSK^{TM}-HD-MW-CNT extraction are compared with those from NOBIAS-chelate PA1 extraction.

normalized patterns to that for the upper continental crust (UCC) [31] (Fig. 7). Generally, the REE concentrations in both data sets were the lowest at the surface and the highest at the thermocline depth. In addition, for both data sets, the UCC normalization patterns showed the general characteristics of REE in the open ocean, i.e., LREE depletion, negative Ce anomaly, and HREE enrichment.

4. Conclusion

This study established the optimized conditions for using MW-CNTs for the analysis of REEs in seawater. These conditions were identified for high-dispersion-type MW-CNTs (HD-MW-CNTs) attached to TSK^{TM} beads. Flow rate, pH, and volume of seawater, as well as eluent type and volume, were considered. We obtained a batch capacity of about 70 mg/g for La with these resins and used a conventional polyethylene column for the pre-concentration of REEs in seawater. For pH 4, 2 mL/min flow rate, 100 mL seawater volume, and 3 mL of 2 M HNO_3 eluent, detection limits using ICP/MS were in the range of 0.016 (Lu) to 0.159 pg/mL (Ce). Actual seawater collected from the East Sea showed characteristic features typically present in seawater such as minimum concentrations at the surface, maximum concentrations in the lower thermocline, negative Ce anomaly, LREE depletion, and HREE enrichment relative to the upper crustal abundances.

Acknowledgment

This study was financially supported by Research Fund of Chungnam National University in 2009. The authors thank to anonymous reviewers and editor for their careful comments.

References

[1] H. Elderfield, M.J. Greaves, Nature 296 (1982) 214.
[2] J. Zhang, Y. Nozaki, Geochim. Cosmochim. Acta 60 (1996) 4631.
[3] S. Hirata, Y. Ishida, M. Aihara, K. Honda, O. Shikino, Anal. Chim. Acta 438 (2001) 205.
[4] M. Murakami, E. Hamanaka, T. Takada, Anal. Lett. 38 (2005) 2449.
[5] B. Wen, X.Q. Shan, S.G. Xu, Analyst 124 (1999) 621.
[6] P. Liang, Y. Liu, L. Guo, Spectrochim. Acta Part B—At. Spectrosc. 60 (2005) 125.
[7] D.S. Alibo, Y. Nozaki, Geochim. Cosmochim. Acta 63 (1999) 363.
[8] D.J. Piepgras, S.B. Jacobsen, Geochim. Cosmochim. Acta 56 (1992) 1851.
[9] M.B. Shabani, T. Akagi, A. Masuda, Anal. Chem. 64 (1992) 737.
[10] M.B. Shabani, T. Akagi, H. Shimizu, A. Masuda, Anal. Chem. 62 (1990) 2709.
[11] I. Kim, S. Kim, G. Kim, Aquat. Geochem. 16 (2010) 611.
[12] T.H. Zhang, X.Q. Shan, R.X. Liu, H.X. Tang, S.Z. Zhang, Anal. Chem. 70 (1998) 3964.
[13] S.G. Ozcan, N. Satiroglu, M. Soylak, Food Chem. Toxicol. 48 (2010) 2401.
[14] C. Lu, F. Su, S. Hu, Appl. Surf. Sci. 254 (2008) 7035.
[15] C.B. Jacobs, M.J. Peairs, B.J. Venton, Anal. Chim. Acta 662 (2010) 105.
[16] A.F. Barbosa, M.G. Segatelli, A.C. Pereira, A.D. Santos, L.T. Kubota, P.O. Luccas, C.R.T. Tarley, Talanta 71 (2007) 1512.
[17] M.J. Greaves, H. Elderfield, G.P. Klinkhammer, Anal. Chim. Acta 218 (1989) 265.
[18] P. Krystyna, TrAC Trends Anal. Chem. 29 (2010) 718.
[19] J. Lee, M. Kim, C.K. Hong, S.E. Shim, Meas. Sci. Technol. 18 (2007) 3707.
[20] K. Shrivas, H.F. Wui, J. Sep. Sci. 31 (2008) 3603.
[21] V. Datsyuk, M. Kalyva, K. Papagelis, J. Parthenios, D. Tasis, A. Siokou, I. Kallitsis, C. Galiotis, Carbon 46 (2008) 833.
[22] Y. Shirazi, M.A. Tofighy, T. Mohammadi, A. Pak, Appl. Surf. Sci. 257 (2011) 7359.
[23] A. Chakrabarti, LCGC North Am. (2009) 52.
[24] O. Byl, J. Liu, J.T. Yates, Langmuir 21 (2005) 4200.
[25] H. Wu, H.Y. Wen, B.P. Han, B.X. Du, J.S. Lu, J.Y. Tian, Microchim. Acta 166 (2009) 41.
[26] A.H. El-Sheikh, J.A. Sweileh, Y.S. Al-Degs, Anal. Chim. Acta 604 (2007) 119.
[27] H. Katsumata, H. Kojima, S. Kaneco, T. Suzuki, K. Ohta, Microchem. J. 96 (2010) 348.
[28] H.M. Yu, W. Sun, M.L. Chen, Y. Tian, J.H. Wang, Chin. J. Anal. Chem. 38 (2010) 1721.
[29] K.J. Orians, E.A. Boyle, Anal. Chim. Acta 282 (1993) 63.
[30] H. Takata, K. Tagami, T. Aono, S. Uchida, At. Spectrosc. 30 (2009) 10.
[31] S.R. Taylor, S.M. Mclennan, Rev. Geophys. 33 (1995) 241.